Publishing House
AKAPIT

COMPUTER METHODS IN MATERIALS SCIENCE

Informatyka w Technologii Materiałów

Vol. 11, 2011, No. 1

INFLUENCE OF INITIAL STATE AND CHEMICAL COMPOSITION ON THE HARDENING AND SOFTENING KINETICS IN HOT METAL FORMING

PHILIPP HAGEMANN*, RUDOLF KAWALLA, WERNER JUNGNICKEL, MATTHIAS SCHMIDTCHEN

Technische Universität Bergakademie Freiberg - Institut für Metallformung, Freiberg, Germany
**Corresponding author: philipp.hagemann@imf.tu-freiberg.de*

Abstract

Materials in hot metal forming are suspended to a series of plastic deformation until they obtain their final shape and geometry. In classical processing routes a sequence of cooling and reheating and therefore phase transformation is settled prior to deformation after solidification. The recent development in process philosophy is the direct linkage of solidification and deformation without an intermediate step of reheating from low temperatures.

Initial states, especially structure and precipitation state, of reheated and direct-cast materials have a substantial impact on performance and behaviour before, during and after deformation, in particular the hardening and softening kinetics. This applies in particular on the micro-alloyed steels, where precipitation state has a markedly dependence on the prehistory.

The influence of the initial state prior to deformation on flow stress, softening kinetics in particular the recrystallisation kinetics, and the precipitation kinetics is shown using the example of several steel grades. Differences in deformation behaviour are also documented with semi empirical models with their specific coefficients.

Key words: direct charging, reheating, softening kinetics, precipitation

1. INTRODUCTION

The development of direct-charging technologies for linking the solidification with immediately following hot deformation started in the late 1980s and early 1990s with CSP (compact strip production) by SMS and ISP (inline strip production) by Arvedi and Siemens and went further on to the newest ESP-Technique (endless strip production) introduced by Arvedi and Siemens VAI (Arvedi & Bianchi, 2003, Arvedi et. al, 2008). The difference between all these technologies for continuous production of hot strip and the conventional hot rolling production line is the changed temperature-time regime as shown in figure 1. The elimination of a reheating process results in shorter production facilities, a decrease in process time and less energy consumption. On the other hand the direct-charging characteristics of the new techniques demand an advanced knowledge and understanding of the subprocesses and occurring effects as well to operate these production lines successfully and prevent unnecessary downtime.

Steels with low to medium amount of alloying elements usually go through two phase transformations during the conventional hot rolling process: first γ/α-transformation while cooling and afterwards the reverse α/γ-transformation while reheating to rolling temperature. Within the new direct-charging methods the first phase transformation occurs at the end or after the rolling sequence instead, leading to

 ISSN 1641-8581

a difference in both, microstructure and mechanical properties of the material. The changed temperature-time regime influences the recrystallisation and the precipitation state also. Micro alloying elements like titanium for example are not completely dissolved in the metal matrix after reheating up to rolling temperature. That leads to a reduction in the amount of precipitations effecting the properties of the finished material, while the Ti-precipitations are fully dissolved prior to hot rolling in a direct-charging line (Kawalla et al, 2010).

the rolling mill plant. Thus no significant temperature drop between solidification and hot rolling occurs. The rolling sequence of an ESP or CSP plant can be simulated with the roughing mill and a three stand finishing mill within the continuous rolling layout. For simulation of more than four rolling passes reversing rolling can be used at the roughing mill stand. Conventional hot rolling processes are simulated by reheating the material either with the integrated conductive furnace or in an electrical furnace and then transferred to the rolling mill. Temperature developments during the procedure were monitored using thermocouples attached to the sample single pass operation and an arrangement of configurable pyrometers. Next to geometrical and mechanical investigations the integrated cooling line allows defined cooling and thermo mechanical treatment of the material after rolling to figure out different properties and material behavior for direct charging and reheating process lines. The time-temperature regime used at the pilot mill plant provides also the basic data for simulation of hot rolling within the Gleeble HDS-V40.

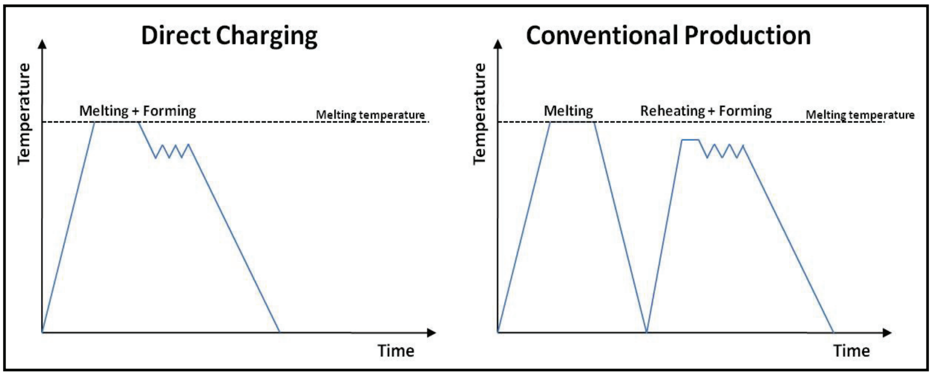

Fig. 1. *Temperature-time-cycles of continues strip production casting (left) and conventional production line (right).*

To consider the influence of both initial states on the behavior and kinetics of the material, a micro-alloyed S355-steel grade with and without Ti as micro alloying element has been investigated. The measured and predicted chemical composition of both steels used is shown in table 1.

Table 1. *Chemical composition of the S355.*

Steel	C	Mn	Si	P	Cr	S	Al	Nb	V	Ti	N
CMn(NbV)	0,048	1,32	0,28	0,016	0,046	<0,0001	0,04	0,043	0,074	0,002	0,0059
CMn(VNbTi)	0,056	1,39	0,25	0,014	0,025	0,0023	0,04	0,037	0,074	0,01	0,0062

2. EXPERIMENTAL PROCEDURE

To investigate the influence of different initial states to the rolling process and the resulting material properties an experimental procedure was developed to simulate a direct charging plant by using the pilot plant for continuous hot rolling at the Institute of Metal Forming, shown in figure 2. Starting point is a steel melt from which a sample with 50 mm height, 80 mm width and 280 mm length is casted in a special mould. After solidification the sample is immediately transferred into an all-side closed thermobox, electrical heated to prevent temperature losses during transport from the melting device to

For simulation of direct charging and conventional rolling processes plane strain compression tests were performed on a Gleeble HDS-V40 forming simulator. The plane strain compression test setup of the Gleeble allows melting of the sample in the deformation zone due to the conductive probe heating in different atmospheres, including air, vacuum and argon gas. Control and guiding of the time-temperature regime was conducted via two platinum thermocouples attached different positions on the sample. Figure 3 shows the Gleeble HDS-V40 and the melting setup in the test chamber (Reip et al, 2007).

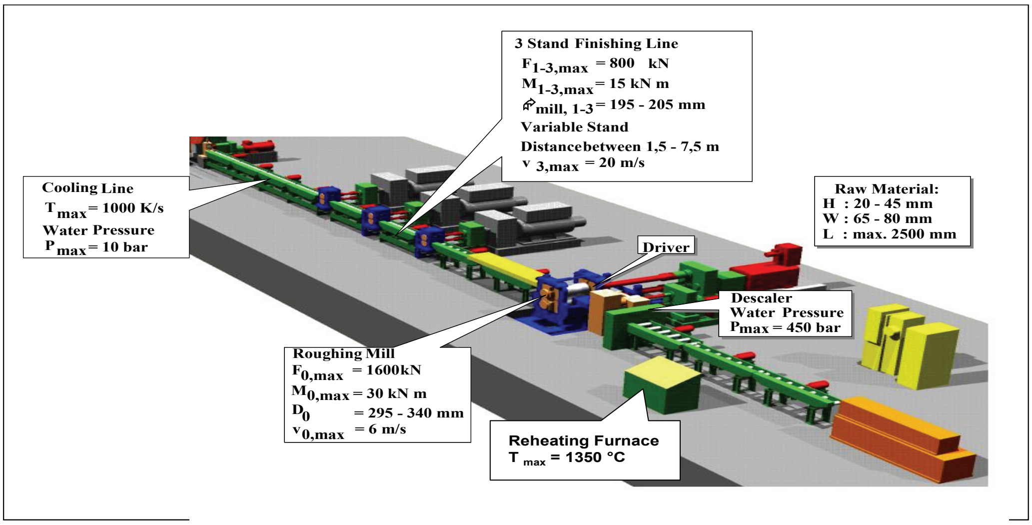

Fig. 2. *Pilot plant at the Institut of Metal Forming for validation.*

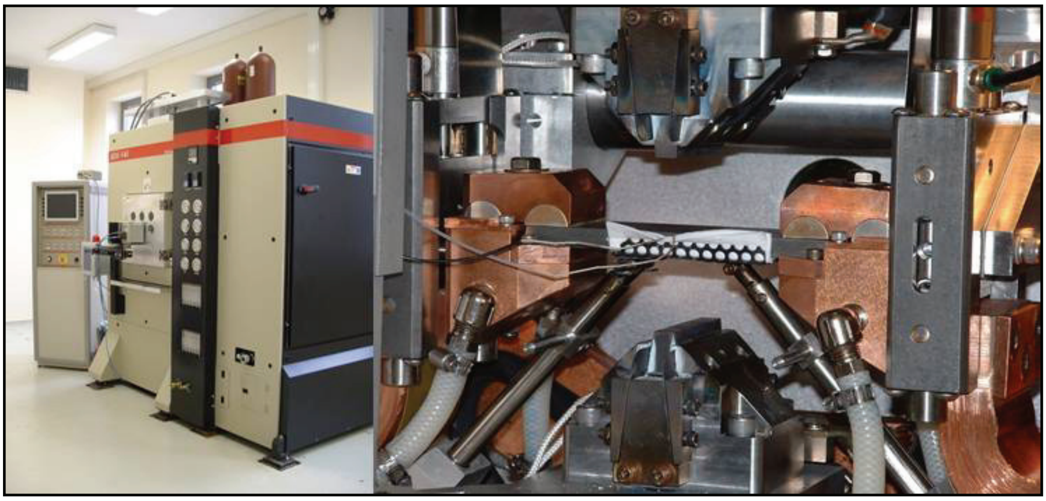

Fig. 3. *Gleeble HDS-V40 (left) and the test chamber with a sample prepared for melting (right).*

Samples for investigation of conventionally rolling procedure were also melted prior to deformation as were done with the direct-charging samples. Different to the direct-charging investigation the sample for conventional rolling were cooled down in the test chamber and then reheated to the desired deformation temperature, ensuring a full two-time phase-transformation.

For the investigation of hardening and softening kinetics, samples were deformed within a two stage plane strain compression test consisting of two defined deformation steps with variable pause times between the deformation steps. The Gleeble HDS V-40 allows controlling and regulating temperature, strain and strain rate during the whole process (Kawalla, 2010). Additional tests were performed to investigate the homogeneity of the temperature field within the deformation zone.

3. RESULTS AND DISCUSSION

For comparison of different initial states due to different rolling techniques only samples of CMb(NbV) steel without titanium were investigated. One set of samples were used to simulate direct-charging while another was used for the conventional hot rolling procedure. For comparison a third set of samples were only reheated to deformation temperature without melting. The different time-temperature regimes and the resulting flow curves are shown in figure 4 (Kawalla et al, 2010).

A significant influence of the hardening and softening behaviour of the steel were predicted on the initial state of the material. The almost identical curves b and c show no effect of the melting within the used setup for simulating the conventional rolling process. Rather the soaking temperature of 1250°C after 10 min setting the initial state in conventional process.

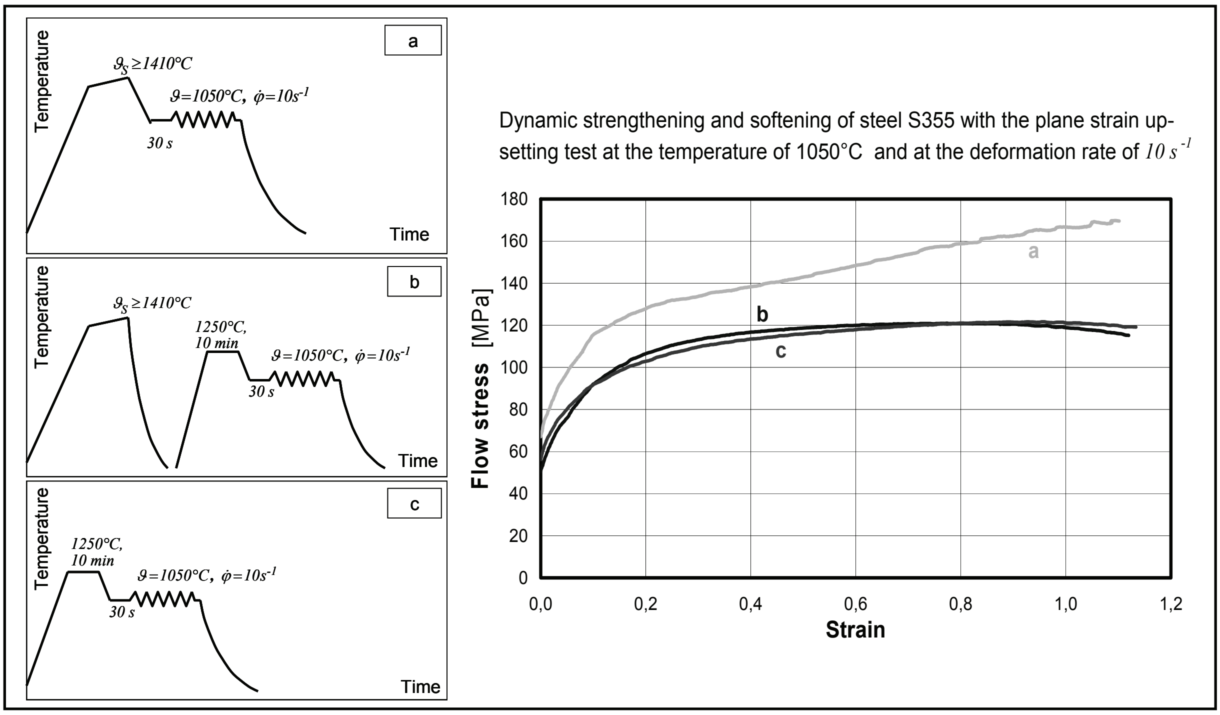

Fig. 4. *Test conditions (left) and flow curves (right) for a) direct charging and b, c) conventional rolling.*

Contrary to this the relation between curve a and b gives a first measure of the effect of direct charging and the differences within the microstructure process. On the basis of this first result static softening kinetics were investigated with the two stage plane strain compression test, where a longer pause time between the deformation steps led to an increase in the amount of static softening and therefore resulted in a decrease of flow stress during the second deformation step. Dynamic recrystallisation didn`t occur in none of the experiments.

The amount of static softening (X_{stat}) can be describe by equation (1), depending on the maximum occurring stress (σ_m), the initial flow stress of the first (σ_{PI}) and second deformation pass (σ_{PII}). Figure 5 is showing the corresponding stress-strain-curve of the two-stage plane strain compression test.

$$X_{stat} = \frac{\sigma_{\max} - \sigma_{PII}}{\sigma_{\max} - \sigma_{PI}} \tag{1}$$

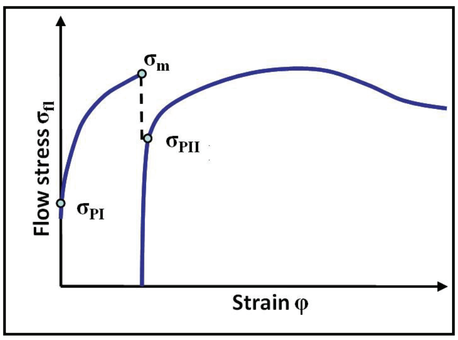

Fig. 5. *Test conditions for double flat compression test.*

Figure 6 gives the fraction of static softening for different initial states and interpass times between the deformation steps. It can be seen, that direct-charging lead to a slowdown in static softening at the same deformation temperature. The different solution states of the micro alloying elements prior to the deformation are responsible for the differences in the static softening behaviour as also already seen for the dynamic softening in figure 4. For the direct-charging material the full content of micro allying elements is dissolved and therefore acting as a barricade for grain boundary migration during the softening processes. The micro alloying element of the reheated material are only partly soluted with the still precipitated fraction not acting as a barrier for the softening kinetics and thus resulting in a speed up for dynamic and static softening.

As thermal activated processes, the softening kinetics increases significantly with rising temperatures for both initial states at the same deformation temperature for both initial states can be stated, that the investigated steel has a high potential for static softening, leading to a softening ratio of more than 2/3 within a pausing time of 10 seconds.

Figure 7 shows the comparison of the static softening kinetics of steel S355 with and without Ti as micro alloying element for direct-charging and reheated material. Prior to the experimental investigations thermodynamic computation were performed to investigate the precipitation states within the samples.

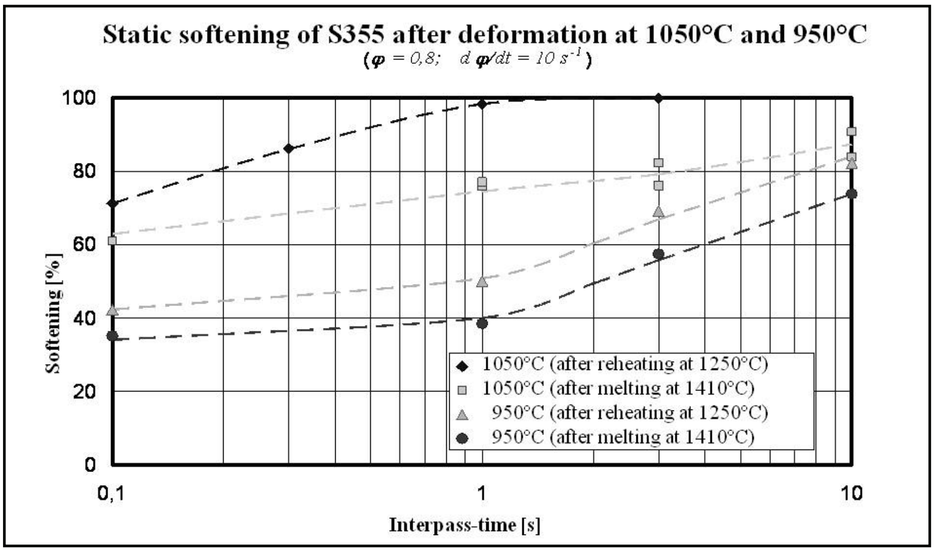

Fig. 6. *Static softening kinetics of the S355.*

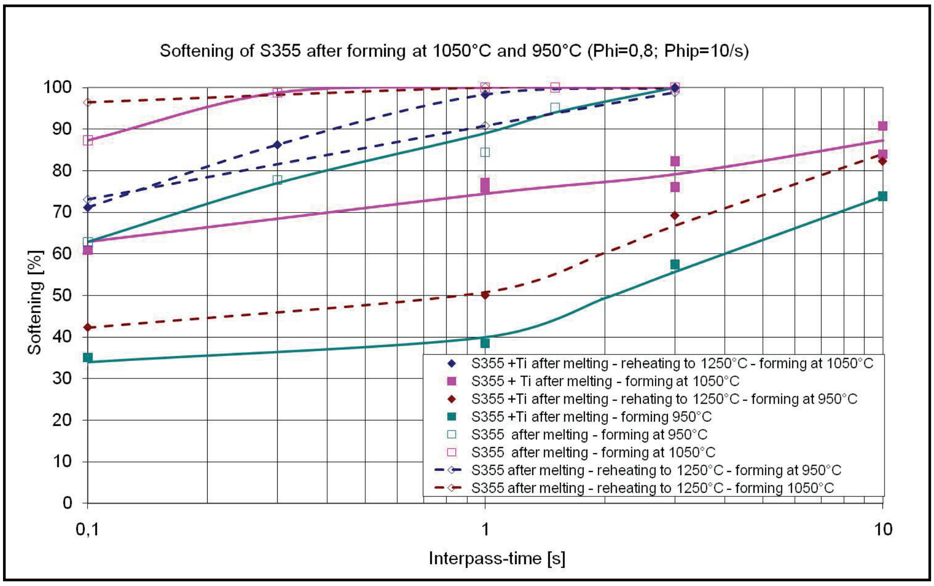

Fig. 7. *Static softening behaviour of both steel grades.*

The results show also the tendency for slowing down of softening kinetics for the direct-charging technique due to the different precipitation state of the micro alloying elements. It is also shown, that the addition of Ti results in noticeably deceleration of the softening kinetics for the same initial state and deformation temperature. This is also consistent with the prior results with more dissolved micro alloying elements after Ti addition restraining the softening processes. In (Reip, 2007) the influenced of the titanium precipitation on the microstructure development is shown.

The results of the two-stage plane strain compression tests were used to calculate the dynamic and static softening amount with the calculations of the JMAK theory. After this theory, the portion of dynamic and static softening can be calculated and lead to the curves in figure 6. The equations out of the JMAK theory for dynamic and static softening are shown in equation (2) and (3) (Krause, 2005) with the correct coefficients for direct charging (2) and conventional production (3). For the investigated steels the deformation is below the critical strain, therefore no dynamic recrystallisation occurs.

$$X_{stat} = 1 - \exp\left(-0{,}693 \left(\frac{t - t_0}{t_{0,5}} \right) \right) \tag{2}$$

$$X_{stat} = 1 - \exp\left(-h_1 \left(\frac{t - t_0}{t_{0,5}} \right)^{0{,}464} \right) \tag{3}$$

The fraction of dynamic softening has to be calculated from flow curves obtained with the first deformation step during the two-stage plane strain compression tests. φ_c is the critical strain for the onset of dynamic softening and $\varphi_{0.5}$ the strain where 50% of dynamic softening is completed, corresponding with the inflection point at the falling flank of the flow curve. For the static softening, t_0 is the time for the onset of static softening after the end of deformation and $t_{0.5}$ is the time where 50% of the static softening is finished.

For static softening, the time when 50% of the material has already softened can be described by equation (4) and (5) with Q_{stat} as the activation energy for static softening. The initial grain size is for direct charging 300 µm (4) and with reheating 140 µm (5).

$$t_{0,5} = 5,604^{-4} \varphi_V^{-0,5} D_0^{1} \dot{\varphi}_v^{-0,501} \exp\left(\frac{200056}{RT}\right) \quad (4)$$

$$t_{0,5} = 4,845^{-8} \varphi_V^{-1,96} D_0^{0,29} \dot{\varphi}_v^{-0,597} \exp\left(\frac{193000}{RT}\right) \quad (5)$$

Another effect which can occur during the two-stage plane strain compression test is the overlapping of hardening and softening effects. Figure 8 shows the results for static softening investigations of the S355 micro alloyed with titanium for different strains for the first deformation step, at 1050°C and a strain rate of $1 s^{-1}$.

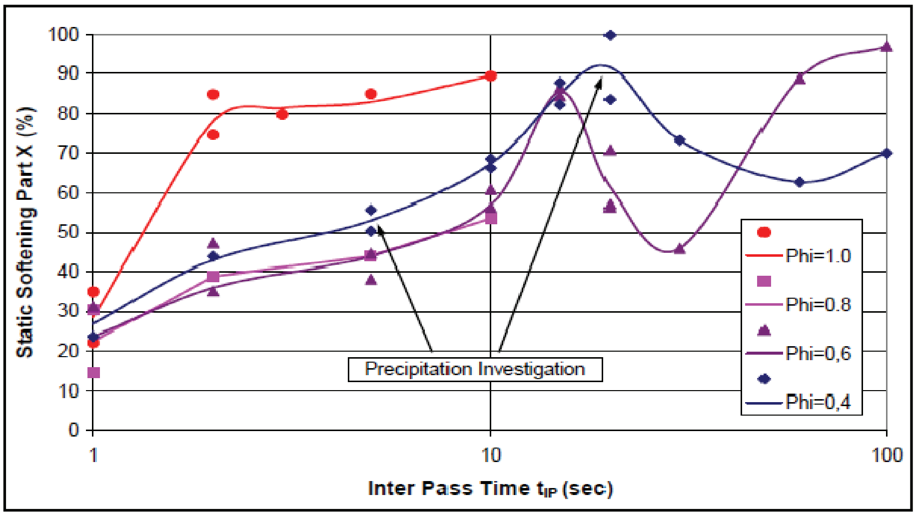

Fig. 8. Strain influence on static softening of CMn(VNbTi).

For the first 10 seconds of inter pass time the typical softening curves similar to figure 6 are obtained. With longer inter pass time a reversing trend can be observed which corresponds the overlapping of the softening processes by hardening processes due to the formation of precipitations. In total two precipitation areas occur. The first area, caused by niobium, is between two and ten seconds for lower strains. In the area after 20s occurs a hardening because of titanium precipitations. The effect goes up to 50s and is overlapped by the softening behavior. The diffusion of titanium in austenite is more slowly than of niobium, so the reaction need more time. This behavior occurs during direct charging and very long interpass times as well as in conventional technologies (Biegus, 1996).

4. CONCLUSIONS

The results obtained show the influence of direct-charging on the dynamic and static softening kinetics. Direct charging leads to higher flow curves due to the missing precipitations in the metal and therefore full efficiency of the fully dissolved micro alloying elements in restraining dynamic and static softening processes. For the conventional rolling process with the intermediate step of cooling and reheating a certain fraction of the containing micro alloying hardening is already precipitated and therefore not longer affecting the softening kinetics. It can be also concluded from the results, that in direct-charging processes a lower content of micro alloying elements is needed for achieving the same effects in restraining static and dynamic softening kinetics and precipitation states after deformation in comparison to the conventional rolling process.

REFERENCES

Arvedi, G., Bianchi, A, 2003, Latest results of Arvedi ISP technology and prospects for the new Arvedi ISP-ECR (endless casting rolling) technology, *Stahl und Eisen*, 123, 3, 57-65.

Arvedi, G., Mazzolari, F., Siegl, J., Holleis, G., Angerbauer, A., 2008, *Acciaieria Arvedi Cremona Works – From ISP to ESP ultimate casting and direct rolling technology*, Rolling Processing Conference.

Biegus, C, 1996, *Anwendung von Werkstoffmodellen auf das Entfestigungsverhalten und die Ferritkorngröße mikrolegierter Baustähle*, Aachen, Shaker.

Kawalla R., Müller W., Jungnickel, W., 2010, Physical Simulation at Hot Deformation, *Material Science Forum*, 638-642, 2591-2597.

Krause, G., Lehmann, G., Gutte, H., Kawalla, R., 2005, *Simulation des Stoffflusses, der Gefügebildung und der Eigenschaftsveränderung für Umformprozesse*, BHT.

Reip, C.-P., Schlüter, J., Kawalla, R., Jungnickel, W., 2007, Softening Kinetics of Microalloyed High-Strength Steel Grades during Hot Forming, *International Conference on Microalloyed Steels*, Pennsylvania, USA.

WPŁYW STANU POCZĄTKOWEGO I SKŁADU CHEMICZNEGO NA KINETYCZNE UMOCNIENIE I MIĘKNIĘCIE W PRZERÓBCE PLASTYCZNE NA GORĄCO

Streszczenie

Materiały kształtowane na gorąco poddawane są kolejnym odkształceniom plastycznym aż do osiągnięcia końcowego kształtu i wymiarów. W klasycznych procesach przeróbki przed rozpoczęciem odkształcenia stosowany jest cykl chłodzenia i nagrzewania, stąd przemiana fazowa występuje pomiędzy krzepnięciem i plastycznym odkształceniem. Połączenie procesów krzepnięcia i odkształcania, bez pośredniego dogrzewania począwszy od niskiej temperatury, jest nową, opracowaną ostatnio technologią. Stan początkowy, a głównie struktura i obecność wydzieleń w materiale dogrzewanym i bezpośrednio po odlaniu, mają istotny wpływ na zachowanie się tego materiału przed, podczas i po odkształcaniu. Wpływ ten jest szczególnie widoczny na kinetykę umocnienia i mięknięcia, przede wszystkim w przypadku stali z mikrododatkami, w których procesy wydzieleniowe zależne od historii procesu odgrywają ważną rolę. W pracy pokazano wyniki badań nad wpływem stanu początkowego materiału na naprężenie uplastyczniające, kinetykę mięknięcia głównie w wyniku rekrystalizacji, oraz na kinetykę procesów wydzieleniowych. Badania wykonano dla kilku gatunków stali. Różnice w zachowaniu odkształcanych stali udokumentowano pół-empirycznymi modelami z dobranymi właściwymi współczynnikami.

Received: September 30, 2010
Received in a revised form: November 2, 2010
Accepted: November 8, 2010